RESEARCH

Open Access

Transient replica symmetry breaking in Brillouin random fiber lasers

Liang Zhang[1*] , Jilin Zhang[1], Fufei Pang[1*], Tingyun Wang[1], Liang Chen[2] and Xiaoyi Bao[2]

*Correspondence:
liangzhang@shu.edu.cn;
ffpang@shu.edu.cn

[1] Key Laboratory of Specialty
Fiber Optics and Optical Access
Networks, Joint International
Research Laboratory of Specialty
Fiber Optics and Advanced
Communication, Shanghai
Institute for Advanced
Communication and Data
Science, Shanghai University,
Shanghai 200444, China
[2] Department of Physics,
University of Ottawa, Ottawa, ON
K1N 6N5, Canada

Abstract

Replica symmetry breaking (RSB), as a featured phase transition between paramagnetic and spin glass state in magnetic systems, has been predicted and validated among random laser-based complex systems, which involves numerous random modes interplayed via gain competition and exhibits disorder-induced frustration for glass behavior. However, the dynamics of RSB phase transition involving micro-state evolution of a photonic complex system have never been well investigated. Here, we report experimental evidence of transient RSB in a Brillouin random fiber laser (BRFL)-based photonic system through high-resolution unveiling of random laser mode landscape based on heterodyne technique. Thanks to the prolonged lifetime of activated random modes in BRFLs, an elaborated mapping of time-dependent statistics of the Parisi overlap parameter in both time and frequency domains was timely resolved, attributing to a compelling analogy between the transient RSB dynamics and the random mode evolution. These findings highlight that BRFL-based systems with the flexible harness of a customized photonic complex platform allow a superb opportunity for time-resolved transient RSB observation, opening new avenues in exploring fundamentals and application of complex systems and nonlinear phenomena.

Keywords: Replica symmetry breaking, Random fiber laser, Brillouin scattering, Rayleigh scattering

Introduction

Compared with conventional lasers, random lasers (RLs) replace mirror-based reflection by random feedback in disorder scattering medium [1], leading to unique laser properties with randomly distributed sharp spikes, *i.e.*, random laser modes, over a broadband pedestal from spontaneous emission. A large number of energetically equivalent random modes introduced in such cavity-free configuration can coexist with strong inter-modal nonlinear coupling through the gain medium and make the system disorder and quenched. The condition in which these separated thermodynamic phases with related random modes dominate dynamics is similar to the complicated free energy surfaces of spin glass with a large number of local minima [2]. Correspondingly, each separated thermodynamic phase is called a pure state [3]. Therefore, RLs involving a large number of competing random modes induced frustration play a non-trivial role as a new photonic platform for the study of complex systems such as spin-glasses behavior. According

to the spin-glass theory by Parisi [4, 5], the transition to a glassy phase is signaled by replica symmetry breaking (RSB), that is, the distribution function of similarity q between every two pure states is the physical order parameter of the spin glass [6, 7]. This Parisi overlap is the order parameter that indicates the transition to an RSB phase dominated by an energetic landscape.

During the last two decades, the presence of Lévy-like fluctuations near the laser threshold has been established as a hallmark of RL systems [8–11], in which the pump power plays the role of inverse temperature in spin glass state in magnetic systems. The RSB with a typical Lévy distribution was experimentally reported for the first time in a random laser employing a functionalized thiophene-based oligomer (T_5OCx) in the amorphous solid state with planar geometry [12]. The connection between the photonic spin-glass phase and the phenomenon of RSB has also been theoretically predicted and experimentally demonstrated in RL systems [13–15]. The statistical physical method is then utilized to analyze the nonlinear dynamic of multimode laser systems with open and irregular cavities [16, 17] as well as RL-disordered systems [18], predicting the dependence of the RSB phase transition on the pump power. Furthermore, the complete phase diagram of the conversion from closed to open cavity is described from the perspective of nonlinearity and disorder, and the RSB phase transition is predicted to appear in the RL system with fluorescence quenching defects [19]. By utilizing the replica method of spin-glass theory, the Parisi overlap between the pulse-to-pulse fluctuations in RLs within a framework of macroscopical observation was carried out whilst its distribution function provides evidence of a transition to a glassy light phase compatible with RSB. Subsequently, the RSB in a variety of RL systems has been discovered, including solid-state lasers [12, 20], dye lasers [21], liquid-state lasers [22], liquid crystal lasers [23], semiconductor lasers [24], fiber lasers [25–29], etc., albeit with omission of any micro-state evolution.

Recently, an elaborated discovery of the correlations between intensity fluctuations in an RL system has been proposed to reveal that the RSB transition is accompanied by stochastic dynamics of the lasing modes, which dominates the competition for gain intertwined with correlation and anti-correlation between random laser modes in this complex photonic phase [29]. Although the universal existence of the RSB in the most random fiber laser systems was confirmed, the underlying physics of such phenomena has never been well investigated. Particularly, random fiber lasers with broadband gain spectra result in a superposition of a large number of random modes with a smooth envelope over a typical bandwidth of more than 0.1 nm (*i.e.*, ∼ 10 GHz), which is usually difficult to be precisely and timely resolved due to limited spectral resolution and slow scanning time. As a result, the elaborate revealing of intrinsic relevance between random laser modes and the display of the RSB is eventually ambiguous, which deserves detailed investigation, especially considering the existence of numerous discrete coherent laser modes in Raman-based random fiber lasers [30].

Brillouin random fiber lasers (BRFLs) utilize the coupled photon-phonon interaction along standard communication silica fibers as gain mechanism with tens of megahertz gain bandwidth, at least three orders of magnitudes lower than that of other broadband gain profiles (*e.g.*, Raman gain profile), leading to coherent random lasing spikes prominently on the top of the Brillouin gain pedestal [31]. The lasing

mode landscapes of the BRFL determined by the superposition of a large number of Brillouin gain-shared Fabry–Perot resonators formed by numerous Rayleigh scatters along optical fibers could fall into a much narrower gain band (*e.g.,*, < 20 MHz in silica fibers), which can be readily captured by the off-the-shelf optoelectronic device. Thanks to the long-term damping effect among the interplayed acoustic phonons and photons as well as phase noise suppression by randomly distributed Rayleigh scattering, random lasing modes in BRFLs exhibit unique characteristics of high temporal coherence and ultra-narrow linewidth down to tens of hertz [32–34]. Meanwhile, BRFLs intrinsically offer abundant spatial–temporal processes and strong stochastic characteristics [35]. Energy coupling and gain competition in random lasing resonance intrinsically allow such a disorder photonic system with different mode landscapes even under the same pump power. Meanwhile, the barrier among these mode landscapes is easy to be broken so that it is uncertain which mode landscape the laser system would be subject to. Ultimately, the BRFL system exhibits the characteristics of the quenched disordered interaction and frustration, benefiting to the observation of the photonic glass behavior [27].

Besides, distributed feedback from a random fiber grating also enables the BRFL with distinct RSB phenomena and correlation of laser fluctuation from Rayleigh scattering [28]. Ultimately, distinct features in BRFL systems typically with over tens of milliseconds long-lifetime random mode landscape not only allow macroscopical observation of photonics spin glass at the onset of the lasing threshold akin to other RL systems, but also highlight an appealing opportunity for high-precision retrieval of real-time random mode dynamics as well as its relevance with the RSB and photonics spin glass above the pump threshold. Spin-glass behavior as well as the RSB observation in BRFL have been reported by revealing power fluctuations in terms of temporal traces [27] and power spectrum density (PSD) of laser radiation [28, 29]. However, all these works conventionally concentrate on the statistics of laser power fluctuations rather than laser modes dynamics, which unfortunately lost the opportunity to reveal the transient dynamics and the generic signature of the BRFL for the RSB occurrence. To this end, high-fidelity retrieval of random laser mode landscapes of the BRFL would be desirable to discover the transient RSB phase transition in terms of relatively long lifetime laser mode metastable states.

In this paper, we experimentally demonstrate the phase transition with the RSB by unveiling time-resolved statistics of a BRFL by means of the optical heterodyne technique, for the first time, to the best of our knowledge. In the BRFL with a few kilometer-long gain and Rayleigh fibers, the dynamics of spectral purified random modes within the time scale from millisecond to second is exquisitely mapped in both temporal and spectral domains. By statistical analysis (*i.e.*, the Parisi overlap q) of BRFL's intensity fluctuation on a large scale of pump power levels, the occurrence of the RSB transition is evidently elaborated with correspondence to random mode landscape evolution. Furthermore, the manipulation of the random mode density by utilization of the longer length fiber for Brillouin gain and Rayleigh scattering media eventually mitigate the coherent time extension of random modes and release the barriers among numerous competing mode landscapes, accounting for the RSB state with higher probability. The findings manifest that BRFLs with striking features of spin-glasses accompanied by

versatile transit dynamics, provide a new paradigm towards the next frontiers exploration of fundamental physics in photonic complex systems and nonlinear phenomena.

Results and discussion

Spin-glass theory of RLs

The concept of RSB was first introduced by G. Parisi to describe disordered magnetic systems [36], which can be used to identify different states from identically-prepared magnetic spin-glass systems under the same conditions. Afterward, the research on this phenomenon was widely extended among plenty of complex photonics systems. Generally speaking, the RSB phenomenon can be specifically characterized by the replica overlap parameter (q), *i.e.*, the statistical distribution of the correlation function of replica samples in a complex photonics system. Consequently, the phase transition of photonic RSB can be indicated by the statistical distribution of replica overlap parameters (q values) during observation time, which is calculated among fluctuations of either intensity in a specific photonic system. Considering the light beam intensity of a photonic system subsequently recorded as I_α, where $\alpha = 1, 2, ..., N_s$ denote the replica labels, the average intensity $\bar{I}(k)$ at a given optical frequency indexed by k is

$$\bar{I}(k) = \frac{1}{N_s} \sum_{\alpha=1}^{N_s} I_\alpha(k).$$

(1)

The intensity fluctuation of each replica can be deduced by:

$$\Delta_\alpha(k) = I_\alpha(k) - \bar{I}(k)$$

(2)

Ultimately, the overlap parameter between two replicas (α and β) is defined as [12], where $\alpha, \beta = 1, 2, ..., Ns$ denote the labels of two replicas and N_s is the total number of replicas.

$$q_{\alpha\beta} = \frac{\sum_k \Delta_\alpha(k) \Delta_\beta(k)}{\sqrt{\left[\sum_k \Delta_\alpha^2(k)\right]\left[\sum_k \Delta_\beta^2(k)\right]}}$$

(3)

In terms of a photonic system of a BRFL, each laser output spectrum can be considered a replica under identical experimental conditions. Through the collection of N_s spectrums, the overlap parameters between two replicas $q_{\alpha\beta}$ can be calculated to determine their distribution $P(q)$. A photonic spin-glass phase with the emergence of the RSB phenomenon is featured by the deviation of the maximum q_{max} to the origin (*i.e.*, $|q_{max}| \neq 0$), which is the analogy to an equilibrium spin-glass phase with RSB appearing in disordered magnets below the critical freezing temperature. Otherwise, the replica remains symmetrical as q_{max} occurs exclusively at $q_{max} = 0$, which reflects that paramagnetic phase with the temporal and spatial disorder at the high temperature. Therefore, the overlap parameter q as well as its distribution is a critical indicator for RSB phenomenon observation in disorder complex systems.

In spite of statistical stability in most disorder complex systems, diverse transient processes indeed exist in photonic disorder systems, such as random lasers with nonlinear gain mechanisms of either Raman [30] or Brillouin scattering [35]. To elaborate

the transient dynamics of such photonic disorder systems, time series analysis of the RSB phenomenon can be implemented via the distribution of the overlap parameters within sequent observation sub-time windows. Specifically, if the sub-time windows are fine enough to be comparable with the characteristic duration of random laser modes dynamics, the transient characteristics (i.e., the transient process of RSB on the time scale) of such a system are expected to be well resolved. Total observation time T is equally divided into N_m groups with sub-time window T_τ, where $\tau = 1, 2, ..., N_m$. Therefore, the overlap parameter between two replicas (α and β) within the sub-time window T_τ is rewritten as,

$$q_{\alpha\beta,\tau} = \frac{\sum_k \Delta_{\alpha,\tau}(k)\Delta_{\beta,\tau}(k)}{\sqrt{\left[\sum_k \Delta_{\alpha,\tau}^2(k)\right]\left[\sum_k \Delta_{\beta,\tau}^2(k)\right]}} \tag{4}$$

Consequently, the temporal evolution of $|q_{max}|(\tau)$ can be hence deduced for further investigation of the transient process of RSB in photonic disorder systems, like a RFL photonic system.

BRFL emission spectrum and measurement

As a proof-of-concept, we exploit a BRFL photonic system, involving nonlinear gain mechanism as well as disorder-induced distributed random feedback in optical fibers, to characterize its statistics for observation of the transient RSB. Distinct from other RL systems, the BRFL eventually exhibits versatile mode landscapes within much narrower gain profiles (*e.g.*, over three orders of magnitudes narrower than that of Raman gain profiles), allowing high-precision retrieval via heterodyne technique with low-speed photon-electron conversion. Meanwhile, the random mode density of BRFLs can be also flexibly manipulated by the implementation of different gain and Rayleigh fiber lengths. In this scenario, both intensity and spectra evolution of the BRFL can be instantaneously resolved by utilizing the optical heterodyne method, offering a straightforward reflection between the laser mode dynamics and replica symmetry (RS) phase. To demonstrate the emergence of RSB in the BRFL system, we analyze the statistical properties of the series of spectral data, including the shot-to-shot correlations of intensity fluctuation. The experimental setup is sketched in Fig. 1 and detailed in Methods.

As illustrated in Fig. 2a, the threshold power P_{th} of the conducted BRFL was measured as 15.64 mW with a slope efficiency of 20.19%. The central wavelength of the Stokes laser is located at 1550.25 nm, showing an optical signal-to-noise ratio of over 35 dB. The beat signals of the pump and Stokes waves with the central frequency of a 10.8-GHz Brillouin frequency shift were converted by a photodetector (PD) and displayed by an electrical signal analyzer (ESA). As shown in Fig. 2b, when the pump power is raised slightly, the noise spectrum around 10.8 GHz caused by spontaneous Brillouin scattering turned to appear within the natural Brillouin bandwidth of $10 \sim 20$ MHz in silica fibers. Remarkably, once the pump power surpassed the laser threshold, the narrow-linewidth laser spikes occurred on the top of the Brillouin gain pedestal, marking the emergence of dominating coherent random laser emission, which coincides with other coherent RLs [37]. Compared with conventional lasers, RLs enabled by the combination of distributed Brillouin gain and Rayleigh scattering disordered feedback unambiguously enrich
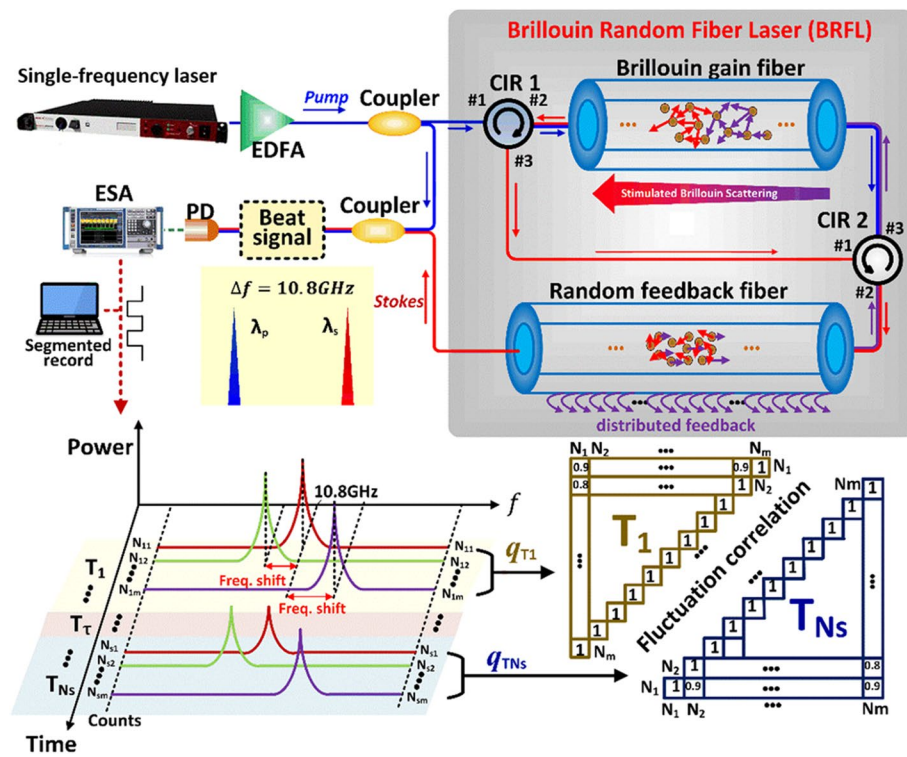
Fig. 1 Schematic for the transient RSB observation and statistical analysis in the BRFL. EDFA—Erbium doped fiber amplifier, CIR—optical fiber circulator, PD – photodetector, ESA—electrical signal analyzer
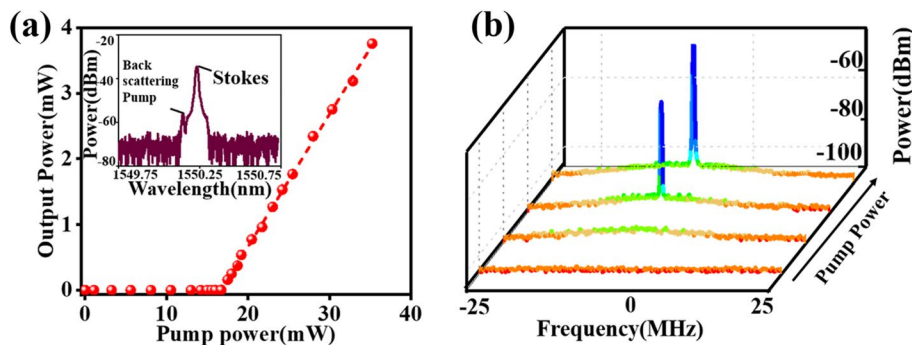

Fig. 2 BRFL emission characteristics. **a** Optical power with respect to the pumping power shows a typical laser threshold behavior ($P_{th} = 15.64$ mW). **b** Beat signals for different pump power ratios ($P/P_{th} = 0.1, 0.8, 1.2, 2.0$), its center frequency was normalized to the Brillouin frequency shift of 10.8-GHz in silica fibers

the diverse physical phenomena and unique statistical characteristics, which offers an intriguing photonic platform for RSB observation.

BRFL statistics with low-spectral resolution metrology

To investigate the thermodynamic behavior of the random lasing modes based on the replica approach according to spin-glass theory, 1000 spectra of the BRFL emission under a low spectral resolution of 100 kHz at every 2 ms over 2 s total time window were obtained under different pump power ratios P/P_{th}, as shown in Fig. 3. It
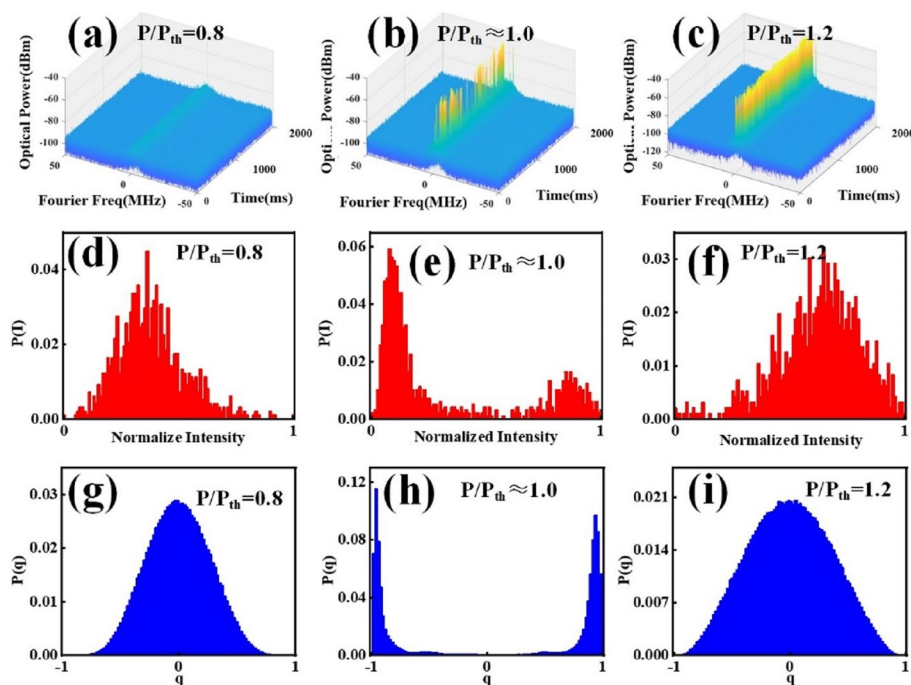
Fig. 3 BRFL for each excitation power in the regimes well below [$P/P_{th} \approx 0.8$], around [$P/P_{th} \approx 1.0$], and above [$P/P_{th} = 1.2$]. **a-c** Spectra of 1000 consecutive shots for each excitation power. **d-f** Intensity distribution calculated from 1000 spectra. **g-i** Distribution $P(q)$ of values of the Parisi overlap parameter q for the same values of the excitation power ratio P/P_{th}

should be pointed out that the RSB actually describes a relatively slow micro-state evolution of a complex system that is observed macroscopically. Thus, the threshold power becomes a slowly varying parameter characterizing the overall random mode competition in the BRFL, therefore the threshold value P_{th} is not purely a function of the environmental perturbation, but is a function of the mode landscape, akin to spin glass. In this scenario, P_{th} could be approximatively estimated as constant in terms of a short observing time window during which the low-frequency environmental disturbance, as well as mode landscape change, could be negligible. We investigated the regimes below, around, and well above the laser threshold. In Fig. 3a, for $P/P_{th} = 0.8$, the intrinsic broadband emission from Brillouin scattering is dominated. As the excitation pump power is around the threshold (15.64 ± 0.80 mW), as shown in Fig. 3b, for $P/P_{th} \approx 1.0$ (see Supplement III for details), a compelling bandwidth narrowing and salient intensity fluctuations took place, which indicated that an optimum resonance paves in the random medium for lasing was locked at the moment. Indeed, when the pump power is above the threshold, strong and narrow-band random spikes exist stably along with much weaker intensity fluctuations, as shown in Fig. 3c. The probability density functions (PDFs) of the intensity values for each pump power are plotted in Fig. 3d-f. The intensity is consistent with Gaussian distribution when the excitation power is below ($P/P_{th} = 0.8$) or above the threshold ($P/P_{th} = 1.2$), which arises as a consequence of the Gaussian-distributed intensity with statistical properties governed by the central limit theorem. When the pump power is around the threshold ($P/P_{th} = 1.0$), the distribution is observed to be in accord with

the heavy-tailed *"L"*-like distribution, which exhibits a much larger variance in the distribution of emitted intensities.

Meanwhile, the set of all value q between every two traces of N samples for each different pump power were calculated from the measured spectra, determining their distribution $P(q)$ which is regarded as the theoretical distribution of the overlap between the replicas for describing the glassy phases. Figure 3g-i illustrate the PDFs of the value-q as increasing the pump power. In Fig. 3g, most values of q muster around zero at low pump power, which means the majority of replica samples are independent. By increasing the pump power to the threshold nearby, the q-value starts to extend to the whole range of values, which manifests the appearance of the replica symmetry breaking. For excitation pulse energies well above the RL threshold, the fluctuations of intensities decline leading to the PDF $P(q)$ starting to return near zero, as shown in Fig. 3i, with a trend to suppress the photonic spin glass phase. In the calculation of the overlap parameter q between the spectra replicas under the low spectral resolution, different output mode landscapes turn out to be indistinguishable (*i.e.*, $q_{max}=0$), making the RSB phase transition unobservable (details can be also found in Method Section and Fig. S9 in the supplementary). Ultimately, the BRFL statistics revealed at low-spectral resolution exhibit the RSB around the pump threshold while preserving the RS phase below or well above the laser threshold, which is in accordance with previous literature typically implemented by traditional optical metrology with the low-spectral resolution (~0.01 nm or 10 GHz) such as optical spectrum analyzer [28, 38].

BRFL statistics with high-spectral resolution metrology.

Subsequently, the spectra of beat signals within 1000 ms were collected by the ESA at a high-spectral resolution of 10 kHz. Figure 4a shows heatmap plots of the BRFL intensity in the domains of time and frequency. The whole observation time window was consecutively divided into 20 sub-time windows for the sake of transient dynamic observation of the BRFL. Distribution $P(q)$ of the Parisi overlap parameter q was calculated from the spectra in each sub-time window and the $|q_{max}|$ were obtained and plotted in Fig. 4b. Figures 4c-d show the overlap distribution $P(q)$ in various sub-time windows containing both RS and RSB phases. The Gaussian distribution of $P(q)$, as shown in Fig. 4c, indicates that the glassy behavior would be suppressed ($q\approx0$) as the BRFL got trapped in one dominating mode that is harder to move out in its neighboring landscape. On the contrary, in the glassy phase, as shown in Fig. 4d, random modes are strongly coupled by the nonlinearity in the random laser system and the random mode landscape can switch to another one which can be thought of as ferromagnetic and anti-ferromagnetic dominated configurations. Each realization tends to fall into one of these two branches so that fluctuations from shot to shot appear either completely correlated ($q\approx1$) or anti-correlated ($q\approx-1$). Note that, considering the balanced trade-off between the spectral resolution and sweeping time, the utilization of the higher spectral resolution will be beneficial to the characterization of the RSB observation in random laser-based complex systems.

Two representative states, steady state (200–400 ms) and RSB phase state (300–500 ms) are selected with an overlap of 100 ms (300–400 ms). Figure 5a displayed the representative emission spectrums from selected shots within the time interval (206 ms,
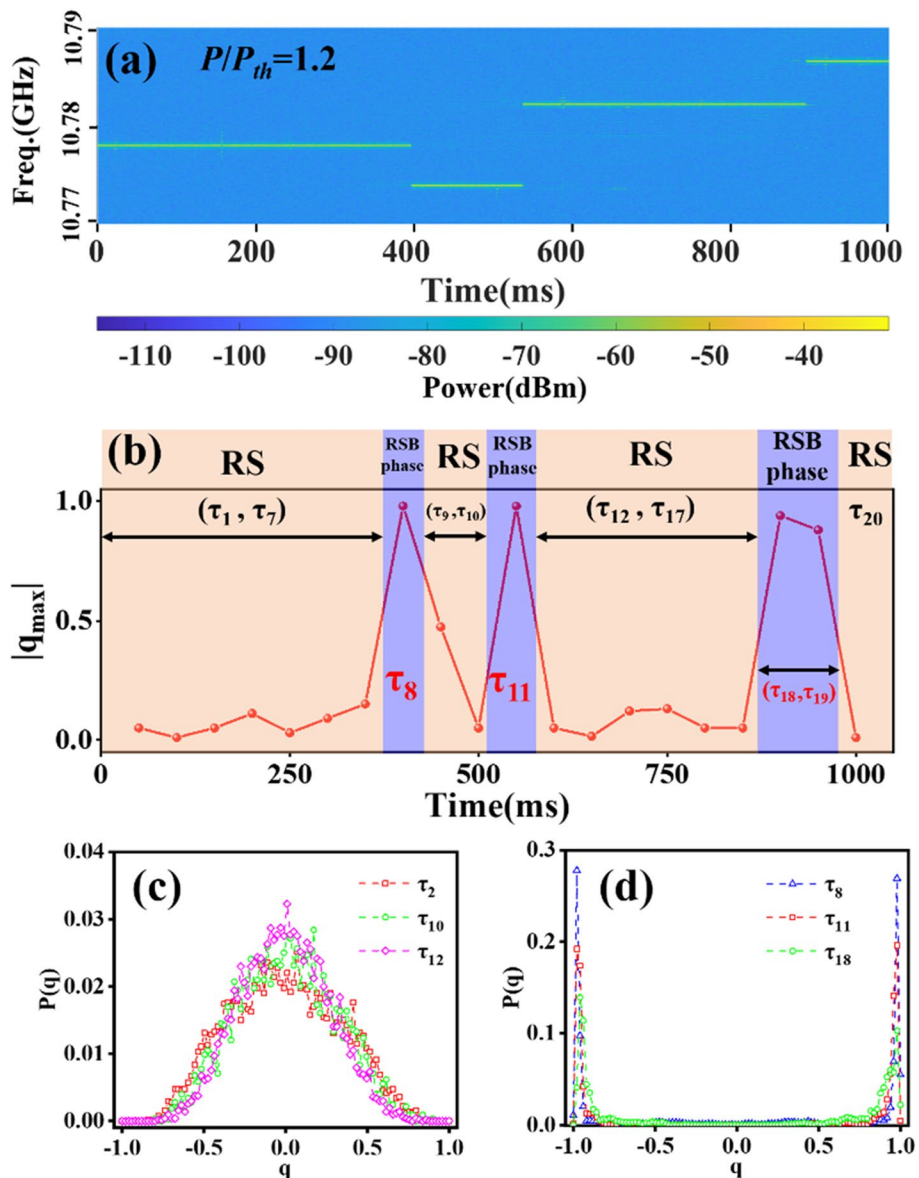
Fig. 4 Time-domain evolution of RSB in the BRFL under $P/P_{th} = 1.2$. **a** The spectra of the beat signal within 1000 ms above the laser threshold. **b** $|q_{max}|$ in 20 subsequent time windows with a time interval of 50 ms. **c** P(q) within sub-time windows of τ_2, τ_{10} and τ_{12}. **d** P(q) within sub-time windows of τ_8, τ_{11} and τ_{18}

300 ms). It can be clearly observed that the shots collected from 200 to 400 ms were similar with weak power fluctuation. Distribution $P(q)$ of values of the Parisi overlap parameter q calculated from the spectrums of the BRFL shown in Fig. 5c. A replica-symmetric phase sets with $P(q)$ distributed around $q = 0$, which is consistent with Gaussian distribution. On the other hand, as shown in the selected shots (406 ms and 418 ms) of Fig. 5b, the main random modes do not remain steady during the measurement time, instead, change stochastically from the former mode to another one reflected in the dynamic alternation of the dominant intensity peak. The energy transfer process from one dominating random mode to another causes a remarkable intensity fluctuation at the corresponding wavelength, which makes the replicas distinguishable and the RSB
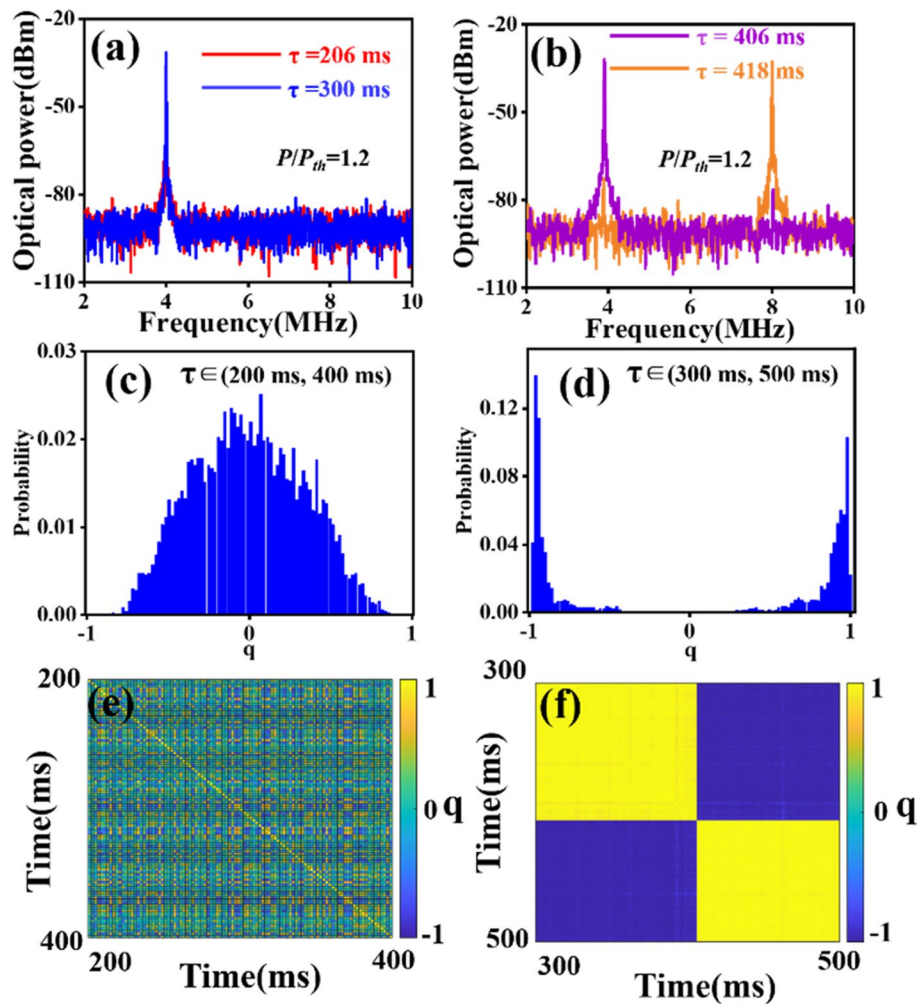
Fig. 5 Correlation analysis of trace-to-trace intensity fluctuation in the BRFL under $P/P_{th} = 1.2$. **a** The representative emission spectrums in the steady state of the BRFL. **b** The representative emission spectra in the RSB phase state. **c** $P(\boldsymbol{q})$ calculated from the spectra in the quasi-steady state within a range of 200–400 ms. **d** Distribution $P(\boldsymbol{q})$ in RSB phase state within the range of 200–400 ms. **e** The map of Parisi overlap parameter $\boldsymbol{q}$ above the laser threshold within a range of 200–400 ms. **f** The map of Parisi overlap parameter $\boldsymbol{q}$ above the laser threshold within the range of 300 -500 ms

observable, as shown in Fig. 5d. The replicas are divided into two pure states, and the distributions of their similarity $P(q)$ are also separated.

The distribution $\boldsymbol{P(q)}$ of the correlation between every two pure states $\boldsymbol{q}$ is the physical order parameter of the spin glass. The Parisi overlap parameter $\boldsymbol{q}$ calculated by Eq. (4) refers to the correlation between intensity fluctuations. Figures 5e and f show heatmap plots of the RBFL with values of the order parameter $\boldsymbol{q}$ representing correlations between intensity fluctuations at different time points T_i and T_j. The color code in green essentially depicts the absence of correlations between intensity fluctuations, whereas yellow ($\boldsymbol{q = 1}$) and blue ($\boldsymbol{q = -1}$) indicate correlated and anti-correlated fluctuations, respectively. During the time window from 200 to 400 ms, containing one dominating random mode, intensity fluctuations of these shots are nearly statistically independent (*i.e.*, almost no correlation), as shown in Fig. 5e. On the contrary, as the time window moved from 300

to 500 ms, the BRFL is undergoing the transformation of mode landscapes. In Fig. 5f, it could be observed the presence of both correlation (yellow) and anti-correlation (blue) in two random modes which intercoupled via gain competition along the Brillouin gain media in the nonlinear regime above the threshold. Most interestingly, the correlation of the same group of shots contained by different time windows was also distinct. The overlap traces (300 ms-400 ms) were uncorrelated (green) with each other in Fig. 5e, but correlated (yellow) in Fig. 5f. Strong intensity-means value change is considered to be the origin of this phenomenon. It suggests that the occasional appearance of the mode hopping in BRFLs inevitably introduces instantaneous drastic intensity changes in average energy, which highlights the RSB phase transition, even at the pump power well above the threshold. In other words, BRFL-based photonic systems not only feature a spin glass phase state at the onset of the laser threshold, akin to other RL systems, but also discriminatively exhibit dynamic evolution of transient alternation between spin glass phase and optical ferromagnetic phase, even above the pump threshold, which is traditionally analogy to the glass transition temperature.

Time-resolved RSB in the BRFL

Figure 6 shows the temporal evolution mapping of q_{max} with respect to different pump power ratios. The quasi-static state dominated over the 400-ms interval when pump power was below the BRFL threshold. With the increase of the pump power around the laser threshold, random laser modes were motivated sporadically and quenched immediately, attaining multiple random mode landscapes. Consequently, the steady state of such a photonic system was broken whilst the RSB phase become the dominant over the whole time window, which was illustrated as green blocks in Fig. 6. Meanwhile, the transition from the RSB to the RS phase around the laser threshold was also observed and the probability of such occurrence is related to the mode density (see Supplement III for details). As the pump power well exceeded the threshold, some or even one dominating
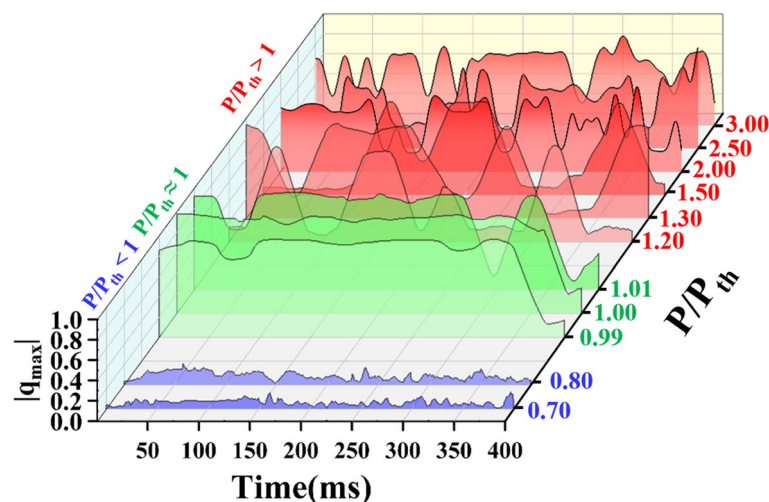

Fig. 6 Temporal evolution of |q_{max}|(400-ms observation time) under different pump power ratios. Three typical pump power regimes: (i) $P/P_{th} < 1$ (blue curves), (ii) $P/P_{th} \approx 1$ around threshold (green curves) and (iii) $P/P_{th} > 1$ (red curves)

random mode would compete and obtain relatively higher gain from photon-phonon coupled interplay for sustaining moderate long photon lifetime due to localization of the photons by amplified scattering over silica fibers. It hence leads to the mode landscape with much-reduced mode density, which is critical to the transient RSB observation of simplified random laser complex systems. Note that, the metastable state duration of this mode landscape could be flexibly harnessed via the manipulation of the fiber lengths in BRFLs, which will be discussed in next section. Typically, thanks to the prolonged coherent time of photons, the mode-switching process between two adjacent mode states in BRFLs could sustain within a duration of milliseconds, leading to transient mode landscape dynamics in the spectral domain and the strong fluctuation of random laser intensity in the time domain. With respect to the pump power around the laser threshold, the presence of the RSB phase with $|q_{max}|=1$ (corresponding to dual-mode landscape) sporadically occurred within the observing time windows until the BRFL statistics returned to the RS phase with $|q_{max}|=0$, as the pump power was well beyond the laser threshold and even the pump power reached three times higher than the laser threshold (see Supplement IV for more measurement in BRFL under high pump power). The transient RSB in BRFL-based photonic systems above the laser threshold, albeit with stochastic emergence, intrinsically features the analogy to dynamic characteristics of spin glass nature with disorder-induced frustration of the lasing random modes from the nonlinear gain of Brillouin scattering and abundant coherent interference of Rayleigh scattered random feedback in optical fibers. Note that, high-order Stokes light in the BRFL can be generated as the pump power is further increased, which is predicted to intentionally produce more disorder signature of laser radiation via stimulated Brillouin scattering (SBS) and Kerr nonlinearities and hence yield the RSB phenomenon [27].

Transient time scale for RSB observation

From the above-mentioned results, two statistical states of both RSB and RS basically coexist in BRFL systems with pump power surpassing the laser threshold in the presence of high spectral resolution and fast enough observation time with respect to the lifetime of the quasi-static mode landscape. To further validate it, two cases of random laser mode status were figured out as its lifetime is longer and shorter than the observation transient time window when the pump power is well-above the threshold (*i.e.*, $P/P_{th}=1.5$). As shown in Fig. 7a, when the duration of one dominating laser mode is
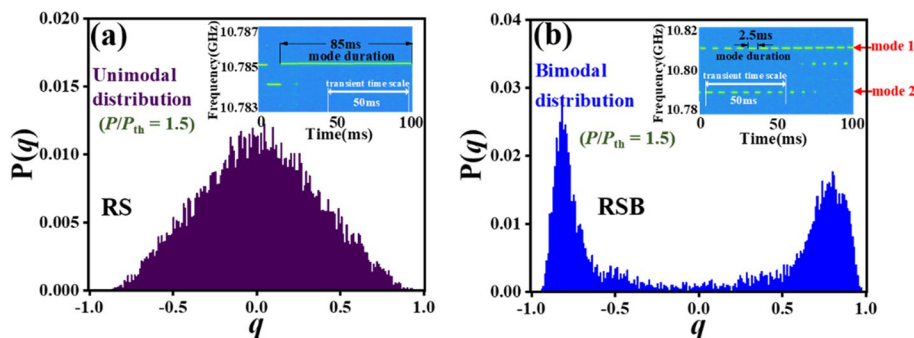

Fig. 7 Distribution of P(q) when $P/P_{th}=1.5$ under the observation time of 50 ms. **a** Unimodal state **b** Bimodal state. The insets correspond the mode evolutions

longer than the observation time window (*i.e.* 50 ms), P(q) exhibits a unimodal distribution representing the RS state. While multiple dominating laser modes with random mode hopping during the observation window corresponds to P(q) with bimodal distribution, which featured the RSB phase transition as the observation time covering the average duration of discrete random modes, as illustrated in Fig. 7b. Consequently, the explicit emergence of the RSB phenomenon in intensity fluctuation of laser above the threshold relies on that the transient observation time window is shorter than the mode duration. On the contrary, the RS preserving of intensity fluctuations above the lasing threshold will only occur when the transient observation time scale is greater than the lifetime of a single dominating random laser mode.

Mode density manipulation in BRFLs for RSB observation

For BRFLs, the random cavity length is an important parameter affecting the laser mode density and the lifetime of localized laser photons. The random feedback Stokes light propagates through several local ring paths in the optical fiber and the superposition of these localized ring cavities would determine such unique properties of the laser. With the increase of the fiber length, ring paths localization of random modes becomes more complex and unpredictable, leading to its vulnerable nature dedicated by both pump and environmental perturbations. As a result, the probability of lasing output switching among different mode landscapes would be increased in the BRFL system, resulting in a decrease of the average lifetime of the output mode landscapes. The spectra of beat signals within 1000 ms with different fiber lengths in BRFLs are illustrated in Fig. 8a-d (see Supplement II for more mode density measurements in BRFLs). When the total fiber length (defined as the sum of the gain and feedback fibers) in the BRFL is 1.5 km, the stable unimodal landscape can basically maintain during the observation time of up to 1000 ms. However, for the BRFL with a fiber length of 9 km, the mode competition among four activated random modes was dominant. In Fig. 8c and d, with the further increase of the BRFL fiber length, the total number of 12 and 40 random modes were excited within the selective observation time scale of 1000 ms, regarding the fiber lengths of 16 and 20 km, respectively. In these scenarios, the transient unimodal landscapes of the BRFL are expected to be remarkably overlapped, predicting a sustainable RSB over the whole observing time scale even at a higher pump power ratio. Correspondingly, the histogram of the random mode number and the mode hopping frequency (inverse proportion to the average mode duration) with respect to the fiber length were characterized, as shown in Fig. 8e and f. As the fiber length increases from 1.5 km to 20 km, the number of random modes increases from 2 to around 40 per unit time. Meanwhile, the average lifetime of random modes decreases from 333.0 ms to 1.1 ms.

Furthermore, the impact of random mode density on the RSB observation is investigated. The heat maps of q distributions with multi-mode BRFL radiation with different random cavity lengths were illustrated in Fig. 9. Multiple random laser modes within the observation time of 1000 ms were used for the calculation of the Parisi overlap parameter q. Random modes can divide replicas into N pure states with a total q-value number of $N(N-1)/2$ between every two pure states, which results in the fractal structure of q distribution in Fig. 9a-d. Compared with the first-order RSB occurrence with only two pure states dominated by two random modes with one q-value, the multi-mode random
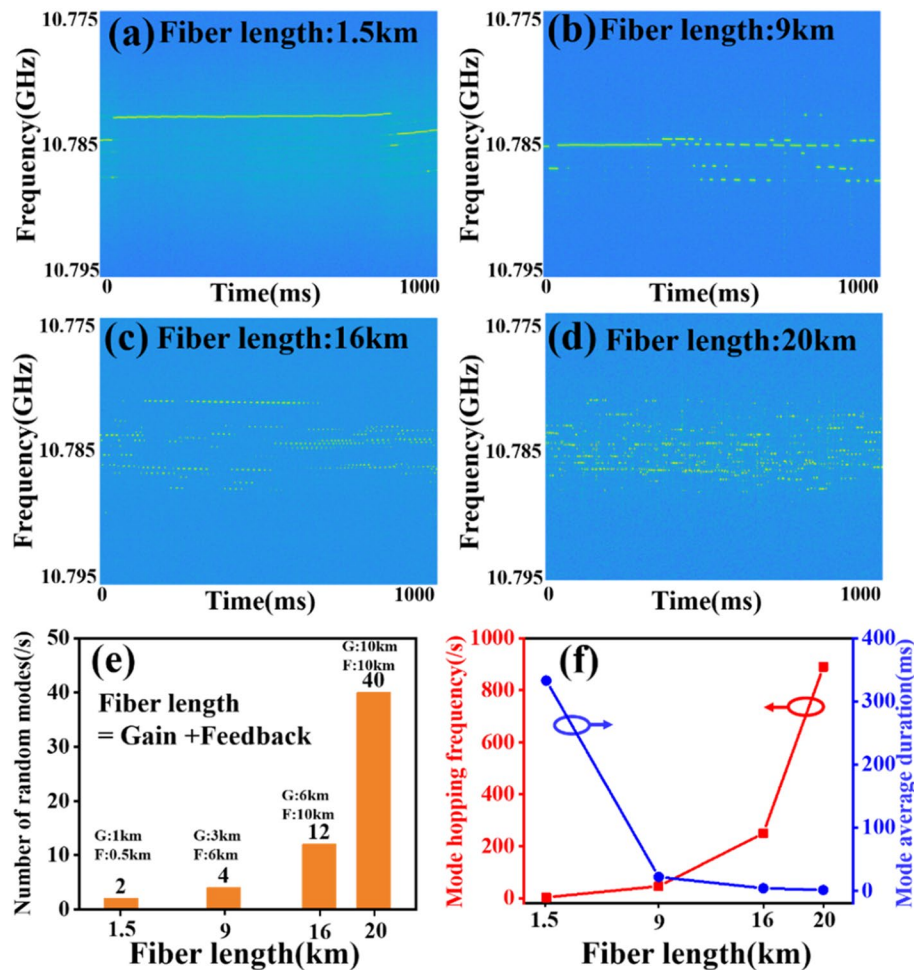
Fig. 8 Mode density manipulation in BRFLs. The spectra of beat signal within 1000 ms with the total fiber length of **a** 1.5 km, **b** 9 km, **c** 15 km, and **d** 20 km; **e** Histogram of the quantity of random modes; **f** average mode during and mode hopping frequency with respect to the fiber length of the BRFL

laser system with a large number of discrete q-values definitely diversifies the complexity of the system as well as the dynamics of the RSB occurrence and even exhibits the signature of higher-order RSB with the fractal structure of the distribution of q. Moreover, it should be noticed that the q-value turns out to be concentrated around the value of 0, as shown in Fig. 9d, which is mainly due to the low sampling rate setting in data acquisition. When the average lifetime of mode landscapes was hundreds of milliseconds in the BRFL system with short fiber (< 10 km), the acquisition with the sampling period of 2 ms was sufficient to record the transient switching process among different mode landscapes. However, the BRFL system with long fiber (> 20 km) is more sensitive to environmental perturbations, resulting in a decrease of the average lifetime of the output mode landscapes, which is even shorter than the sampling time period. In this situation, the acquisition of a low sampling rate cannot capture the phase transition process, leading to the unobservability of transient RSB phenomenon. To address this issue, the utilization of a modified optical heterodyne method with the down-converted beat signal frequency can be adopted. For instance, an off-the-shelf electro-opto
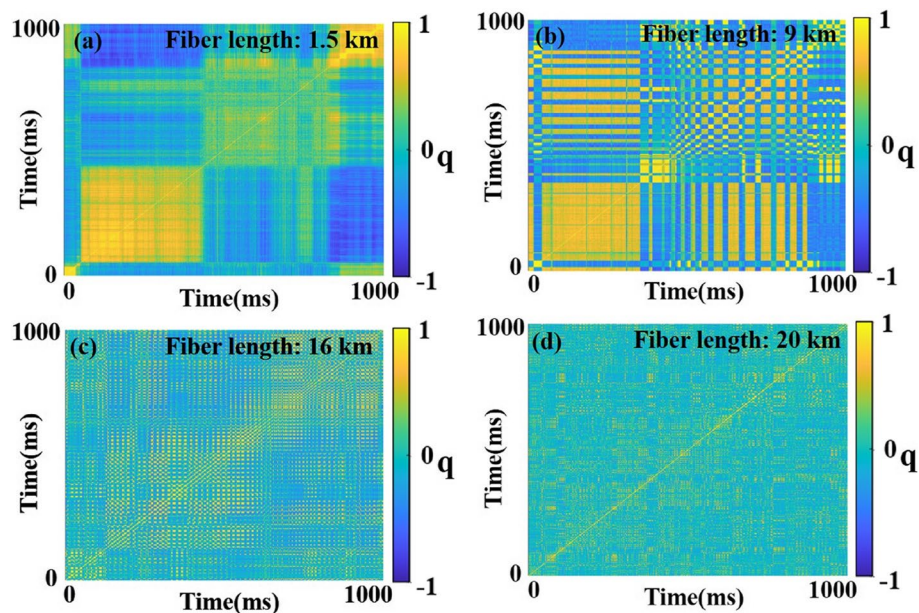
Fig. 9 The *q* distribution of BRFL spectrum with different modes density determined by different fiber lengths of **a** 1.5 km, **b** 9 km, **c** 16 km and **d** 20 km

modulator can be used to generate the sideband of the pump as the local reference for beating with Stokes laser by down-converting the center frequency from 10.8 GHz to even tens of MHz, which can be readily captured by a photodetector (*e.g.*, 100 MHz bandwidth) and an oscilloscope (OSC) for replicas data acquisition with a high-enough sampling rate. Besides, several factors in spectrum measurement influence the transient RSB observation in RFL systems, (1) resolution: the spectral resolution needs to be at least high enough to distinguish any two or more random modes; (2) time scale: the observation time scale should be large to include multiple random modes; (3) pump power: the pump power is required to be higher for activation of one or even more order of Stokes random lasing emission. It finds that the disordered complexity of BRFL-based photonic systems with unambiguous dependence of mode density on the fiber length would highlight a compelling opportunity to flexibly harness a customized BRFL-based photonic complex platform for underlying physics exploration of time-resolved transient RSB observation.

Conclusions

To summarize, the transient RSB is experimentally demonstrated in a BRFL-based photonic platform. With the aid of the optical heterodyne technique, the random laser modes are accurately retrieved with both temporal and spectral dynamics, attributing to the RSB phase transition as the pump powersurpasses the laser threshold. The manipulation of random mode density can be facilitated via the flexible selection of different-scale Brillouin gain and Rayleigh feedback fibers, benefiting the explicit analogy between the RSB phase transition and the mode dynamic evolution of BRFLs in a time-resolved manner. The BRFL-based photonics systems, involving nonlinear gain mechanism as well as disorder-induced stochastics, are believed to manifest typical spin-glass features, which

opens new avenues in exploring fundamental physics for complex systems and nonlinear phenomena, such as turbulent-like behavior [39, 40] and extreme events [41, 42].

Method

Experimental setup

Figure 1 shows the schematic of the real-time observation of replica symmetry breaking in a BRFL and the random lasing radiation. A single-frequency laser (Koheras Adjustik E15, NKT) with a center wavelength of 1550.183 nm was amplified by an Erbium-doped fiber amplifier (EDFA) and then injected into a random fiber laser configuration through an optical fiber circulator (CIR 1) as the pump source for the BRFL. With a delayed self-heterodyne interferometer, the 3-dB linewidth of the pump laser source was characterized as 627 Hz. A spool of 3-km single mode fibers (SMFs) was serving as the Brillouin gain medium while another spool of 6-km SMFs was utilized to provide distributed Rayleigh scattered random feedback, which was recirculated through another optical fiber circulator (CIR 2) back to the Brillouin gain fiber. By increasing the pump power, the backward Stokes waves were generated and then boosted via longitudinal acoustic wave coupled SBS interaction. After passing through the port #2 of the CIR 2, the backscattered Stokes light was launched through the 6-km SMF and then partially reflected by Rayleigh scattering from the refractive index inhomogeneity along the long-span silica fibers. Such distributed Rayleigh scattered Stokes light as random feedback can be circulated back to the Brillouin gain fiber through the CIR 2 for random lasing resonance.

Laser intensity measurements

The beat RF signals between Stokes and pump light were converted by a high-speed photodetector with a bandwidth of 20-GHz, which definitely covers the heterodyne beat signals with a typical center frequency of ~ 10.8 GHz (corresponding to the Brillouin frequency shift of the silica fibers). Then, the beat signals were finally digitized by either an ESA or an OSC in terms of spectral resolution requirement. The frequency span of 20 MHz is selected to collect all random modes within the typical Brillouin gain bandwidth, which basically guarantees the high-fidelity observation of the RSB in BRFLs. The spectrum evolution is subsequently acquired in segments under the drive control of designed external trigger signals for further time-series analysis of the overlap parameters q_{max} (τ). As shown in the bottom part of Fig. 1, the evolution of the spectrum was initially collected during the whole observation time scale which was then divided into *Ns* segments, and each sub-time segment was successively labeled as T_1, T_2,..., T_{Ns}. In each sub-time segment, random lasing spectra with total number of N_m were collected, and then the Parisi overlap parameter $q_{\alpha\beta}$ (α, β = 1,2, ..., N_m) between every two spectra can be obtained. Therefore, the total number $N_m(N_m-1)/2$ of Parisi overlap parameter $q_{\alpha\beta}$ can be then plotted as the heat maps to visually observe the fluctuation correlation of each replica and then be used for q statistics analysis in each sub-segment. Subsequently, **Ns** groups of the q distribution, labeled as q_{T_1}, q_{T_2}, . . . , $q_{T_{Ns}}$, can be obtained, which reflects the time-dependent signature of glassy behavior in photonic systems. Furthermore, each segment corresponds to a tiny time window comparable to the mode switching period, which is the necessary preprocessing for transient analysis of RSB transition.

Abbreviations

RL	Random laser
BRFL	Brillouin random fiber laser
RSB	Replica symmetry breaking
RS	Replica symmetry
PD	Photodetector
ESA	Electrical signal analyzer
PDF	Probability density function
EDFA	Erbium-doped fiber amplifier
SMF	Single mode fiber
CIR	Optical fiber circulator
OSC	Oscilloscope

Supplementary Information

The online version contains supplementary material available at https://doi.org/10.1186/s43074-023-00107-2.

> **Additional file 1: Fig. S1.** Temporal traces of the BRFL emission. (a) The BRFL waveform within 10 ms time scale. (b) and (c) represent the waveform zoom in the red/blue boxes, respectively. (d) and (e) represent the corresponding spectra of (b) and (c). (f) 2D heat map of BRFL traces within 10 ms corresponding to (a). **Fig. S2.** The BRFL lasing spectrum evolution within 1000 ms by employing different lengths of gain and feedback fibers. Fixed 3-km gain fiber with different lengths of feedback fiber (a) 1 km, (b) 6 km, and (c) 10 km. Fixed 10-km feedback fiber with different lengths of gain fiber (d) 3 km, (e) 6 km, and (f) 10 km. **Fig. S3.** The histogram of random modes number (red) and mode hopping frequency (blue) in BRFL. (a) fix the 3-km gain fiber with different lengths of feedback fiber (1 km, 6 km 10 km). (b) fix the 10-km feedback fiber with different lengths of gain fiber (3 km, 6 km 10 km). **Fig. S4.** Spectrum evolution of Brillouin RFL around threshold (a) PP =14.84 mW (b) PP=16.44 mW. **Fig. S5.** (a) The evolution of BRFL spectrum pumped around threshold within 400 ms. (b) the evolution of q_{max} within 400 ms. **Fig. S6.** The spectrum of the BRFL and the temporal evolution of Parisi overlap parameter q when P/Pth = 3.0. **Fig. S7.** The setup of the BRFL with the 3-km gain fiber and 6-km Rayleigh fiber for monitoring the high-order Stokes at three outports (i), (ii), and (iii). **Fig. S8.** High-order Stokes monitoring of the BRFL with the 3-km SMF gain fiber and 6-km SMF Rayleigh fiber at P/Pth=4.0. (a), (b), (c) represent the spectra monitored at ports (i), (ii) and (iii), respectively. **Fig. S9.** Comparison of the RSB observation in the BRFL at P/Pth=1.8 with different spectral resolutions of (a) 1 MHz and (c) 20 kHz. (b) and (d) represent the q distribution with the observation time scale of 100 ms corresponding to (a) and (c), respectively.

Availability of data and materials
The datasets used and/or analyzed during the current study are available from the corresponding author on reasonable request.

Declarations

Competing interests
The authors declare that they have no competing interests.

References

1. Letokhov VS. Generation of light by a scattering medium with negative resonance absorption. Soviet J Exp Theor Phys. 1968;26:835–40.
2. Thouless D, Anderson P, Palmer RG. Solution of a "solvable model of a spin glass." Phil Mag. 1977;35:593–601.
3. Parisi G. Order parameter for spin-glasses. Phys Rev Lett. 1983;50:1946–8.
4. Parisi G. Infinite number of order parameters for spin-glasses. Phys Rev Lett. 1979;43:1754–6.
5. Parisi G. The order parameter for spin glasses: a function on the interval 0–1. J Phys A: Math Gen. 1980;13:1101–12.
6. Mezard M, Parisi G, Sourlas N, et al. Nature of the spin-glass phase. Phys Rev Lett. 1984;52:1156–9.

7.   Parisi G. Replica theory and spin glasses. In: Krzakala F, editor. Statistical Physics, Optimization, Inference, and Message-Passing Algorithms: Lecture Notes of the Les Houches School of Physics: Special Issue, October 2013. Oxford: Oxford Academic; 2016. https://doi.org/10.1093/acprof:oso/9780198743736.003.0003.

8.   Uppu R, Mujumdar S. Lévy exponents as universal identifiers of threshold and criticality in random lasers. Phys Rev A. 2014;90: 025801.

9.   Lepri S, Cavalieri S, Oppo GL, Wiersma D. Statistical regimes of random laser fluctuations. Phys Rev A. 2006;75: 063820.

10. Uppu R, Tiwari AK, Mujumdar S. Identification of statistical regimes and crossovers in coherent random laser emission. Opt Lett. 2012;37:662–4.

11. Araújo C, Gomes A, Raposo E. Lévy statistics and the glassy behavior of light in random fiber lasers. Appl Sci. 2017;7:644.

12. Ghofraniha N, Viola I, Maria FD, Barbarella G, Gigli G, Leuzzi L, Conti C. Experimental evidence of replica symmetry breaking in random lasers. Nat Commun. 2015;6:6058.

13. Leuzzi L, Conti C, Folli V, Angelani L, Ruocco G. Phase diagram and complexity of mode-locked lasers: from order to disorder. Phys Rev Lett. 2009;102: 083901.

14. Conti C, Leuzzi L. Complexity of waves in nonlinear disordered media. Phys Rev. 2011;83: 134204.

15. Antenucci F, Crisanti A, Ibáñez-Berganza M, Marruzzo A, Leuzzi L. Statistical mechanics models for multimode lasers and random lasers. Phil Mag. 2016;96:704–31.

16. Angelani L, Conti C, Ruocco G, Zamponi F. Glassy behavior of light. Phys Rev Lett. 2006;96(6): 065702.

17. Antenucci F, Crisanti A, Leuzzi L. Complex spherical 2+ 4 spin glass: A model for nonlinear optics in random media. Phys Rev A. 2015;91: 053816.

18. Angelani L, Conti C, Ruocco G, Zamponi F. Glassy behavior of light in random lasers. Phys Rev B. 2006;74: 104207.

19. Antenucci F, Conti C, Crisanti A, Leuzzi L. General phase diagram of multimodal ordered and disordered lasers in closed and open cavities. Phys Rev Lett. 2015;114: 043901.

20. Moura AL, Pincheira PI, Reyna AS, Raposo EP, Gomes AS, de Araújo CB. Replica symmetry breaking in the photonic ferromagnetic-like spontaneous mode-locking phase of a multimode Nd: YAG laser. Phys Rev Lett. 2017;119: 163902.

21. Pincheira PI, Silva AF, Fewo SI, Carreño SJ, Moura AL, Raposo EP, de Araújo CB. Observation of photonic paramagnetic to spin-glass transition in a specially designed TiO_2 particle-based dye-colloidal random laser. Opt Lett. 2016;41:3459–62.

22. Basak S, Blanco A, López C. Large fluctuations at the lasing threshold of solid-and liquid-state dye lasers. Sci Rep. 2016;6:1–8.

23. Kong J, He J, Zhang J, Ma J, Xie K, Chen J, Hu Z. Replica Symmetry Breaking in Cholesteric Liquid Crystal Bandgap Lasing. Ann Phys. 2021;533:2000328.

24. Lima BC, Tovar P, Von Der Weid JP. Generalized extreme-value distribution of maximum intensities and Lévy-like behavior in an SOA-based random feedback laser emission. J Opt Soc Am B. 2020;37:987–92.

25. Lima BC, Pincheira PI, Raposo EP, Menezes LDS, de Araújo CB, Gomes AS, Kashyap R. Extreme-value statistics of intensities in a cw-pumped random fiber laser. Phys Rev A. 2017;96: 013834.

26. Li J, Wu H, Wang Z, Lin S, Lu C, Raposo EP, Rao Y. Lévy spectral intensity statistics in a Raman random fiber laser. Opt Lett. 2019;44:2799–802.

27. Tehranchi A, Kashyap R. Theoretical investigations of power fluctuations statistics in Brillouin erbium-doped fiber lasers. Opt Express. 2019;27:37508–15.

28. Zhou Z, Chen L, Bao X. High efficiency Brillouin random fiber laser with replica symmetry breaking enabled by random fiber grating. Opt Express. 2021;29:6532–41.

29. Coronel E, Das A, González IR, Gomes AS, Margulis W, Von Der Weid JP, Raposo EP. Evaluation of Pearson correlation coefficient and Parisi parameter of replica symmetry breaking in a hybrid electronically addressable random fiber laser. Opt Express. 2021;29:24422–33.

30. Sugavanam S, Sorokina M, Churkin DV. Spectral correlations in a random distributed feedback fiber laser. Nat Commun. 2017;8:1–8.

31. Pang M, Bao X, Chen L. Observation of narrow linewidth spikes in the coherent Brillouin random fiber laser. Opt Lett. 2013;38:1866–8.

32. Pang M, Xie S, Bao X, Zhou DP, Lu Y, Chen L. Rayleigh scattering-assisted narrow linewidth Brillouin lasing in cascaded fiber. Opt Lett. 2012;37:3129–31.

33. Xu Y, Xiang D, Ou Z, Lu P, Bao X. Random Fabry-Perot resonator-based sub-kHz Brillouin fiber laser to improve spectral resolution in linewidth measurement. Opt Lett. 2015;40:1920–3.

34. Saxena B, Ou Z, Bao X, Chen L. Low frequency-noise random fiber laser with bidirectional SBS and Rayleigh feedback. IEEE Photonics Technol Lett. 2014;27:490–3.

35. Tovar P, von der Weid JP. Dynamic Evolution of Narrow Spectral Modes in Stochastic Brillouin Random Fiber Lasers. IEEE Photonics Technol Lett. 2021;33:1471–4.

36. Mezard M, Parisi G, Virasoro MA. Spin glass theory and beyond. Phys Today. 1988;41(12):109–10. https://doi.org/10.1063/1.2811676.

37. Sarkar A, Bhaktha BS. Replica symmetry breaking in coherent and incoherent random lasing modes. Opt Lett. 2021;46:5169–72.

38. Gomes AS, Raposo EP, Moura AL, Fewo SI, Pincheira PI, Jerez V, de Araújo CB. Observation of Lévy distribution and replica symmetry breaking in random lasers from a single set of measurements. Sci Rep. 2016;6:1–8.

39. González IR, Lima BC, Pincheira PI, Brum AA, Macêdo A, Vasconcelos GL, Kashyap R. Turbulence hierarchy in a random fiber laser. Nat Commun. 2017;8:1–8.

40. González I. R., Raposo E. P., Macêdo A., De S Menezes L. & Gomes A. S. Coexistence of turbulence-like and glassy behaviours in a photonic system. Sci Rep. 2018;8:1–8.

41. Xu J, Wu J, Ye J, Song J, Yao B, Zhang H, Rao Y. Optical rogue wave in random fiber laser. Photonics Res. 2020;8:1–7.

42. Kolpakov S, Sergeyev SV, Udalcovs A, Pang X, Ozolins O, Schatz R, Popov S. Optical rogue waves in coupled fiber Raman lasers. Opt Lett. 2020;45:4726–9.

Publisher's Note